Dimethyl and Cationic 1,4-Diazabutadiene Complexes of Platinum(II)

Kaiyuan Yang, Rene J. Lachicotte, and Richard Eisenberg*

Department of Chemistry, University of Rochester, Rochester, New York 14627

Received June 29, 1998

The reaction of the 1,4-diazabutadiene ligand glyoxal bis(2-(methoxymethyl)-4,6-di-*tert*-butylphenyl)diimine (**L**) with the platinum complex $Pt_2Me_4(SMe_2)_2$ yields two isomers of the complex $PtMe_2$**L** (**2a**,**b**) that have been isolated and characterized. The isomers exhibit distorted-square-planar coordination geometries about the central Pt(II) ion and differ only in the relative orientation of the methoxymethyl and *tert*-butyl substituents with respect to the coordination plane of the complex. Isomerization between **2a** and **2b** is promoted by heating solutions of either form of the complex in benzene or chloroform. Upon prolonged refluxing in chloroform, **2a**,**b** react with chloroform to yield the methyl chloro derivative PtMeCl**L**, which is also obtained as syn and anti isomers (**3a**,**b**). Cationic solvento complexes $[PtMe(S)\mathbf{L}]BF_4$ (**4** and **5**, S = MeCN, pyridine) are generated by halide abstraction from **3** using $AgBF_4$. In the presence of selected olefins such as ethylene and acrylonitrile, halide abstraction from **3** by $AgBF_4$ or methyl group abstraction from **2a** and **2b** by the strong Lewis acid $B(C_6F_5)_3$ yields the cationic α-olefin complexes $[PtMe(CH_2CHR)\mathbf{L}]^+$ (R = H, CN; **6** and **7** for the BF_4 salt, **8** and **9** for the $MeB(C_6F_5)_3$ salt). All new compounds have been characterized by IR and NMR spectroscopy. Molecular structures of **2a**,**b**, and **3a** were determined by X-ray single-crystal diffraction.

Introduction

Interest in electrophilic complexes of Pt(II) has been stimulated by the activity of such systems in bond activation reactions and the relevance of these systems as models for catalytically active Pd analogues in polymerization and copolymerization reactions.[1−15] With regard to the former, cationic Pt(II) methyl complexes have recently been shown by Bercaw[2,3] and by Goldberg[4] to effect intermolecular alkane C−H bond activation. These observations build on the seminal work of Shilov[16,17] and subsequent studies by others of chloroaquoplatinum-catalyzed H/D exchange and oxidation reactions in acidic media.[5−9,18] The cationic Pt methyl complexes used in the recent C−H bond activation studies were generated from the corresponding neutral dimethyl complexes by reaction with either the strong Brønsted acid $(HOEt_2)[B(3,5\text{-}C_6H_3(CF_3)_2)_4]$[2,3] or the strong Lewis acid $B(C_6F_5)_3$.[19,20] For Pt(II) complexes, the latter was originally applied by Puddephatt to the demethylation of $PtMe_2$(dbbpy) (dbbpy = di-*tert*-butylbipyridine), which in the presence of CO yielded $[PtMe(CO)(dbbpy)]^+$.[19,20]

The electrophilic Pd complexes that were reported by Brookhart in 1996[10−12] to be active catalysts for α-olefin polymerization are closely related cationic systems of the general formula $[PdMe(L)]^+(B(Ar^f)_4)$, where L is a diazabutadiene (DAB) ligand having 2,6-disubstituted aryl groups on the imine N atoms and $B(Ar^f)_4$ represents one of several noncoordinating borate anions having (fluoroalkyl)phenyl or fluoroaryl substituents. Brookhart's reports follow earlier studies on the electrophilic behavior of cationic Pd(II) systems and their role in ethylene/CO copolymerization.[15] In this catalysis, it is

(1) Periana, R. A.; Taube, D. J.; Gamble, S.; Taube, H.; Satoh, T.; Fujii, H. *Science* **1998**, *280*, 560−564.
(2) Holtcamp, M. W.; Labinger, J. A.; Bercaw, J. E. *J. Am. Chem. Soc.* **1997**, *119*, 848−849.
(3) Holtcamp, M. W.; Neling, L. M.; Day, M. W.; Labinger, J. A.; Bercaw, J. E. *Inorg. Chim. Acta* **1998**, *270*, 467−478.
(4) Wick, D. D.; Goldberg, K. I. *J. Am. Chem. Soc.* **1997**, *119*, 10235−10236.
(5) Luinstra, G. A.; Wang, L.; Stahl, S. S.; Labinger, J. A.; Bercaw, J. E. *Organometallics* **1994**, *13*, 755−756.
(6) Labinger, J. A.; Herring, A. M.; Lyon, D. K.; Luinstra, G. A.; Bercaw, J. E. *Organometallics* **1993**, *12*, 895−905.
(7) Luinstra, G. A.; Wang, L.; Stahl, S. S.; Labinger, J. A.; Bercaw, J. E. *J. Organomet. Chem.* **1995**, *504*, 75−91.
(8) Holtcamp, M. W.; Labinger, J. A.; Bercaw, J. E. *Inorg. Chim. Acta* **1997**, *265*, 117−125.
(9) Stahl, S. S.; Labinger, J. A.; Bercaw, J. E. *J. Am. Chem. Soc.* **1996**, *118*, 5961−5976.
(10) Rix, F. C.; Brookhart, M.; White, P. S. *J. Am. Chem. Soc.* **1996**, *118*, 4746−4764.
(11) Mecking, S.; Johnson, L. K.; Wang, L.; Brookhart, M. *J. Am. Chem. Soc.* **1998**, *120*, 888−899.
(12) Johnson, L. K.; Killian, C. M.; Brookhart, M. *J. Am. Chem. Soc.* **1995**, *117*, 6414−6415.
(13) Kacker, S.; Sen, A. *J. Am. Chem. Soc.* **1997**, *119*, 10028−10033.
(14) Vrieze, K.; Groen, J. H.; Delis, J. G. P.; Elsevier: C. J.; van Leeuwen, P. W. N. M. *New J. Chem.* **1997**, *21*, 807−813.
(15) Drent, E.; Budzelaar, P. H. M. *Chem. Rev.* **1996**, *96*, 663−681.
(16) Goldshleger, N. F.; Eskova, V. V.; Shilov, A. E.; Shteinmann, A. A. *Zh. Fiz. Khim.* **1972**, *46*, 1353.
(17) Kushch, K. A.; Lavrushko, V. V.; Misharin, Y. S.; Moravsky, A. P.; Shilov, A. E. *New J. Chem.* **1983**, *7*, 729.
(18) Hutson, A. C.; Lin, M.; Basickes, N.; Sen, A. *J. Organomet. Chem.* **1995**, *504*, 69−74.
(19) Hill, G. S.; Manojlovic-Muir, L.; Muir, K. W.; Puddephatt, R. J. *Organometallics* **1997**, *16*, 525−530.
(20) Hill, G. S.; Rendina, L. M.; Puddephatt, R. J. *J. Chem. Soc., Dalton Trans.* **1996**, 1809−1813.

10.1021/om980551m CCC: $15.00
Publication on Web 10/22/1998

postulated that two adjacent coordination positions of the catalyst are needed to effect the repetitive addition/insertion sequence of the reaction. Other DAB complexes of Pt and Pd have been reported over the past decade,[21−25] and recently Elsevier has described rigid derivatives of these ligands having aryl imino groups, together with their Pd and Pt dimethyl complexes.[24] With respect to the latter, studies of RX oxidative addition to yield the Pt(IV) and Pd(IV) complexes were conducted with subsequent reductive elimination slowed or inhibited by the rigidity of the particular diazabutadiene employed.

Recently, we described the synthesis of the bulky DAB ligand **L**, in which there are different substituents in the 2- and 6-positions of the arylimino groups, and the dichloro Pt(II) and Pd(II) complexes of **L**.[26] Two isomers

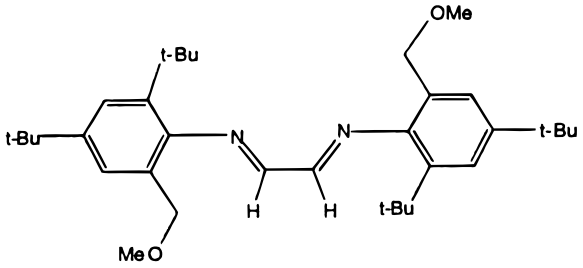

L

of each complex were observed, and structural studies showed them to be syn (**1a**) and anti (**1b**) with respect to the orientation of the aryl substituents relative to the coordination plane. The isomers thus possess mirror

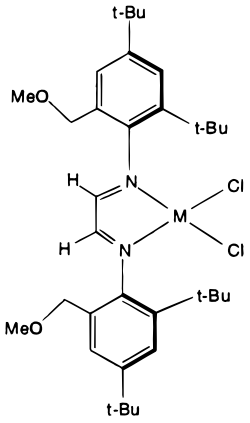

1a

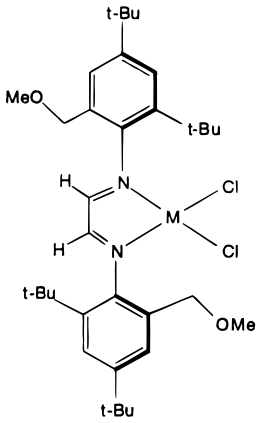

1b

plane and C_2 rotational symmetry, respectively. As part of an effort to examine the electrophilic behavior of Pt(II) complexes containing **L** and to generate selected catalysts having C_2 symmetry, we have synthesized the dimethyl complex $PtMe_2$**L** (**2**) and studied its structure and reaction chemistry. The complex and its corresponding chloro methyl analogue serve as convenient precursors to the formation of cationic methyl derivatives which are stable models of catalytically interesting Pd DAB systems.

Results and Discussion

Synthesis of $PtMe_2$L. The reaction of $Pt_2Me_4(SMe_2)_2$ and the diazabutadiene ligand **L** in a 1:2 ratio was initially investigated in dichloromethane and acetone solutions at both ambient room temperature and solvent reflux conditions. Deep green solutions are obtained in each case, with spectroscopic evidence of two different products. Spectroscopic characterization, elemental analyses, and subsequent single-crystal X-ray diffraction studies (vide infra) of the products show them to be isomerically related forms of the dimethyl complex $PtMe_2$**L** (**2**), as shown in eq 1. Examination of the green

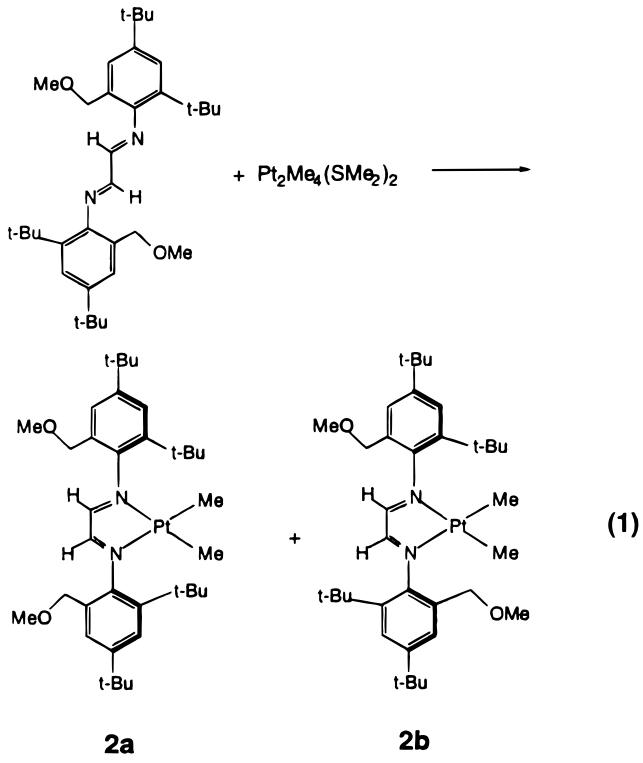

2a **2b** (1)

reaction solutions by ^{1}H NMR spectroscopy showed that the ratio of the two isomers differs with temperature. For example, in acetone solution at ambient room temperature, a 4:1 ratio of the isomers exists, whereas under refluxing conditions the ratio changes to 3:2. Also seen in the ^{1}H NMR spectra of the reaction solutions were resonances of free ligand **L**, in part because of partial decomposition of the starting complex $Pt_2Me_4(SMe_2)_2$, as evidenced by precipitate formation and generation of a black mirror under reflux conditions.

Separation of the product isomers **2a**,**b** in these initial experiments proved difficult by thin-layer chromatography (TLC), since both of the isomers and the free ligand have similar solubility properties and R_f values.

(21) Van Koten, G.; Vrieze, K. *Adv. Organomet. Chem.* **1982**, *21*, 151−239.
(22) van der Poel, H.; van Koten, G.; Vrieze, K. *Inorg. Chem.* **1980**, *19*, 1145.
(23) van der Poel, H.; van Koten, G.; Kokkes, M.; Stam, C. H. *Inorg. Chem.* **1981**, *20*, 2941−2956.
(24) van Asselt, R.; Rijnberg, E.; Elsevier, C. J. *Organometallics* **1994**, *13*, 706−720.
(25) Groen, J. H.; Delis, J. G. P.; van Leeuwen, W. N. M.; Vrieze, K. *Organometallics* **1997**, *16*, 68−77.
(26) Yang, K.; Lachicotte, R. J.; Eisenberg, R. *Organometallics* **1997**, *16*, 5234−5243.

Table 1. Selected ^{1}H NMR Spectral Data for All New Complexes

compd	^{1}H NMR (δ)[a]
2a	2.27 (s, J_{Pt-H} = 40.0 Hz, 3H, $PtCH_3$), 3.23 (s, 6H, OCH_3), 4.62 (d, J_{H-H} = 12 Hz, 2H, CH_aH), 4.97 (d, J_{H-H} = 12 Hz, 2H, CH_bH), 8.79 (s, 2H, NCH)
2b	2.24 (s, J_{Pt-H} = 40.0 Hz, 3H, $PtCH_3$), 3.33 (s, 6H, OCH_3), 4.70 (d, J_{H-H} = 12 Hz, 2H, CH_aH), 4.92 (d, J_{H-H} = 12 Hz, 2H, CH_bH), 8.73 (s, 2H, NCH)
3a	2.02 (s, J_{Pt-H} = 41.2 Hz, 3H, $PtCH_3$), 3.20 (s, 3H, OCH_3), 3.21 (s, 3H, OCH_3), 4.51 (d, J_{H-H} = 11.6 Hz, 1H, CH_aH), 4.55 (d, J_{H-H} = 11.6 Hz, 1H, CH_bH), 4.82 (d, J_{H-H} = 11.6 Hz, 1H, CH_cH), 5.29 (d, J_{H-H} = 11.6 Hz, 1H, CH_dH), 7.91 (s, 1H, NCH_a), 8.56 (s, 1H, NCH_b)
3b	2.00 (s, J_{Pt-H} = 40.8 Hz, 3H, $PtCH_3$), 3.17 (s, 3H, OCH_3), 3.18 (s, 3H, OCH_3), 4.56 (d, J_{H-H} = 11.6 Hz, 1H, CH_aH), 4.59 (d, J_{H-H} = 11.6 Hz, 1H, CH_bH), 4.81 (d, J_{H-H} = 11.6 Hz, 1H, CH_cH), 5.20 (d, J_{H-H} = 11.6 Hz, 1H, CH_dH), 7.81 (s, 1H, NCH_a), 8.45 (s, 1H, NCH_b)
4	0.79 (s, J_{PtH} = 38.8 Hz, 3H, $PtCH_3$), 0.80 (s, J_{PtH} = 36.8 Hz, 3H, $PtCH_3$), 2.03 (s, $NCCH_3$), 2.04 (s, $NCCH_3$), 3.29 (s, 3H, OCH_3), 3.34 (s, 3H, OCH_3), 3.36 (s, 3H, OCH_3), 3.38 (s, 3H, OCH_3), 4.29−4.79 (m, 8H, CH_2), 9.00 (s, 1H, NCH), 9.01 (s, 1H, NCH), 9.06 (s, 2H, NCH)
5	0.90 (s, J_{Pt-H} = 35.6 Hz, 3H, $PtCH_3$), 0.92 (s, J_{Pt-H} = 33.2 Hz, 3H, $PtCH_3$), 3.33 (s, 3H, OCH_3), 3.37 (s, 3H, OCH_3), 3.49 (s, 3H, OCH_3), 3.70 (s, 3H, OCH_3), 4.44−4.90 (m, 8H, CH_2), 9.13 (s, 1H, NCH), 9.14 (s, 1H, NCH), 9.22 (s, 2H, NCH)
6	0.40 (s, J_{Pt-H} = 32.8 Hz, 3H, $PtCH_3$), 0.41 (s, J_{Pt-H} = 34.4 Hz, 3H, $PtCH_3$), 3.31 (s, 3H, OCH_3), 3.36 (s, 3H, OCH_3), 3.38 (s, 3H, OCH_3), 3.42 (s, 3H, OCH_3), 3.93−4.74 (m, 12H, ethylene and benzylic), 9.13 (s, J_{Pt-H} = 32.8 Hz, 2H, NCH), 9.15 (s, J_{Pt-H} = 32.8 Hz, 2H, NCH)
7	0.78 (s, J_{Pt-H} = 46.0 Hz, 3H, $PtCH_3$), 0.80 (s, J_{Pt-H} = 42.8 Hz, 3H, $PtCH_3$), 3.28 (s, 3H, OCH_3), 3.32 (s, 3H, OCH_3), 3.34 (s, 3H, OCH_3), 3.36 (s, 3H, OCH_3), 4.31−4.79 (m, 12H, CH_2), 5.66−5.72 (m, 4 H), 6.22 (d, J_{H-H} = 12 Hz, 1H), 6.23 (d, J_{H-H} = 12 Hz, 1H), 9.05 (s, 1H, NCH), 9.06 (s, 1H, NCH), 9.22 (s, 2H, NCH)
8	0.49 (s, J_{Pt-H} = 30.0 Hz, 3H, $PtCH_3$), 0.52 (s, J_{Pt-H} = 26.4 Hz, 3H, $PtCH_3$), 3.27 (s, 3H, OCH_3), 3.28 (s, 3H, OCH_3), 3.29 (s, 3H, OCH_3), 3.31 (s, 3H, OCH_3), 3.90−4.90 (m, 8H, CH_2), 8.76 (b, 3H, NCH), 8.80 (s, 1H, NCH)
9	0.91 (s, J_{Pt-H} = 42.0 Hz, 3H, $PtCH_3$), 0.92 (s, J_{Pt-H} = 38.4 Hz, 3H, $PtCH_3$), 3.28 (s, 3H, OCH_3), 3.29 (s, 3H, OCH_3), 3.31 (s, 3H, OCH_3), 3.32 (s, 3H, OCH_3), 4.21−5.10 (m, 8H, CH_2), 5.60 (m, 2H), 6.22 (d, J_{H-H} = 12 Hz, 2H), 6.23 (d, J_{H-H} = 12 Hz, 2H), 8.80 (s, 2H, NCH), 8.82 (s, 2H, NCH)

[a] All ^{1}H NMR were recorded in C_6D_6 (**2** and **3**) and $CDCl_3$ solutions (**4**−**9**). Chemical shift values are reported in ppm. Abbreviations: s, singlet; d, doublet; m, multiplet; b, broad.

Table 2. Selected ^{13}C NMR Spectral Data for New Complexes 2−7

compd	^{13}C NMR (δ)[a]
2a	−15.4 (Pt−Me, J_{Pt-C} = 410.0 Hz), 58.0 (OMe), 71.4 (CH_2), 164.8 (NCCN)
2b	−15.2 (Pt−Me, J_{Pt-C} = 403.5 Hz), 58.4 (OMe), 71.7 (CH_2), 164.6 (NCCN)
3a	−11.7 (Pt−Me), 57.8 (OMe), 58.3 (OMe), 71.0 (CH_2), 71.1 (CH_2), 165.7 (NCCN), 166.7 (NCCN)
3b	−11.6 (Pt−Me), 58.2 (OMe), 58.6 (OMe), 72.4 (CH_2), 72.6 (CH_2), 165.3 (NCCN), 166.5 (NCCN)
4	−11.9 (Pt−Me, J_{Pt-C} = 339.1 Hz), 58.0 (MeO), 58.1 (OMe), 58.2 (OMe), 58.4 (OMe), 71.4 (CH_2), 71.5 (CH_2), 71.5 (CH_2), 71.6 (CH_2), 119.2 (MeCN), 167.9 (NCCN), 168.0 (NCCN), 175.6 (NCCN), 175.9 (NCCN)
6	−5.5 (Pt−Me, J_{Pt-C} = 340.0 Hz), −5.6 (Pt−Me, J_{Pt-C} = 334.5 Hz), 57.7 (MeO), 57.9 (OMe), 58.3 (OMe), 58.4 (OMe), 71.29 (CH_2), 71.32 (CH_2), 72.0 (2C, CH_2), 170.0 (NCCN), 170.2 (NCCN), 177.3 (NCCN), 177.4 (NCCN)
7[b]	−11.7 (Pt−Me, J_{Pt-C} = 339.1 Hz), 57.9 (OMe), 58.1 (OMe), 58.2 (OMe), 58.3 (OMe), 71.0 (CH_2), 71.2 (2C, CH_2), 71.6 (CH_2), 105.2 (2C, CH_2**C**HCN), 117.4 (1C, CH_2CH**C**N), 117.5 (1C, CH_2CH**C**N), 144.2 (2C, **C**H_2CHCN), 168.5 (NCCN), 168.6 (NCCN), 176.2 (NCCN), 176.8 (NCCN)

[a] All ^{13}C NMR were recorded in $CDCl_3$ solutions. Chemical shift values are reported in ppm. [b] Assignments for the acrylonitrile resonances are based on the ^{1}H-coupled ^{13}C spectrum and the attached proton test for free acrylonitrile.

The dimethyl complex **2** was also found to decompose slowly on the TLC plate, making rapid separation a necessity. Two adjustments were therefore made in the experimental procedure to facilitate product isomer separation. First, the starting ratio of reactants was changed in order to have no free **L** in solution at the time of product isolation and separation. Second, Me_2S generated upon the reaction shown in eq 1 was removed after 24 h by evacuating all volatiles; subsequent redissolution of the reaction system allowed it to proceed more rapidly to completion. The final separation was performed on a silica gel column using a 9:1 mixture of CH_2Cl_2 and hexane to give **2b** as the first green band and **2a** as the second green band. As seen for the analogous dichloro complex isomers **1a**,**b**, the syn isomer **2a** is slightly more polar than anti isomer **2b**, leading to slower elution of the former.

The ^{1}H NMR spectra of **2a**,**b**, as well as those of other complexes described in the paper, are summarized in Table 1. In benzene-d_6, the ^{1}H NMR spectra of **2a**,**b** show only minor differences, with $PtMe_2$ resonances at δ 2.27 and δ 2.24, respectively, and the same $^2J_{Pt-H}$ coupling constant of 40.0 Hz. The diasterotopic benzylic protons for both isomers exhibit AB coupling patterns that appear as two doublets centered at δ 4.62 and 4.97 for **2a** and at δ 4.33 and 5.16 for **2b**, with the same coupling constant J_{H-H} of 12 Hz for each doublet. Compared to the free ligand L, the diimine proton resonances for **2a**,**b** are shifted to lower field by ~0.5 ppm, which is opposite to the trend observed for the dichloro derivatives $PtCl_2$**L**. The isolability of the two isomers of **2** results from the greatly hindered rotation about the C(aryl)−N bonds arising from the steric repulsions between aryl ring ortho substituents and the metal−diimine chelate.

In Table 2, ^{13}C NMR spectroscopic data for the complexes are presented. In $CDCl_3$ **2a**,**b** give very similar spectra with $PtMe_2$ resonances at δ −15.4 and −15.2, respectively, and J_{Pt-C} coupling constants of 410.0 and 403.5 Hz. The observed chemical shifts for the Pt-coordinated methyl resonances of **2** are comparable to those in other dimethylplatinum complexes reported in the literature. In addition to the $PtMe_2$ resonances, the diimine carbon resonances are seen at δ 164.8 for **2a** and δ 164.6 for **2b**, which are ca. 1 ppm to lower field relative to the free ligand **L**.

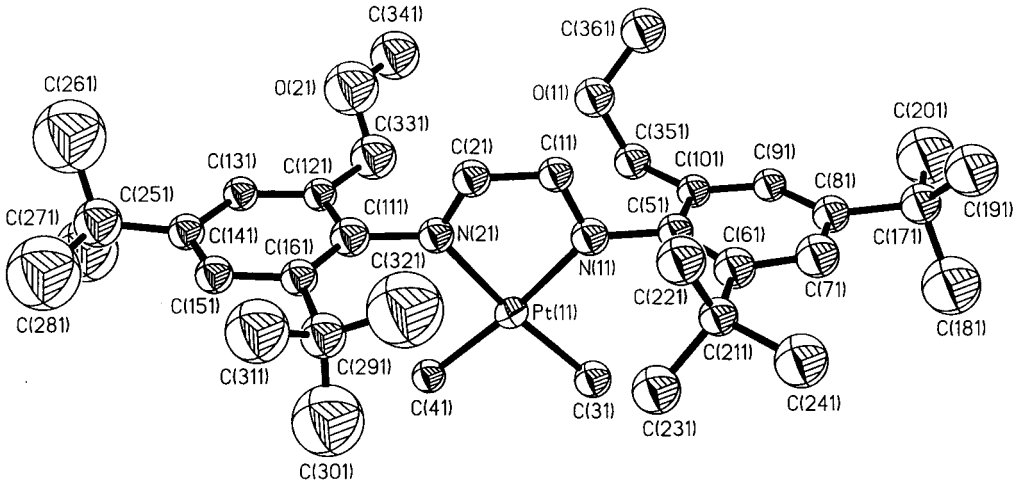

Figure 1. ORTEP diagram of **2a**. Thermal ellipsoids are shown at 50% probability. Hydrogen atoms are omitted for clarity.

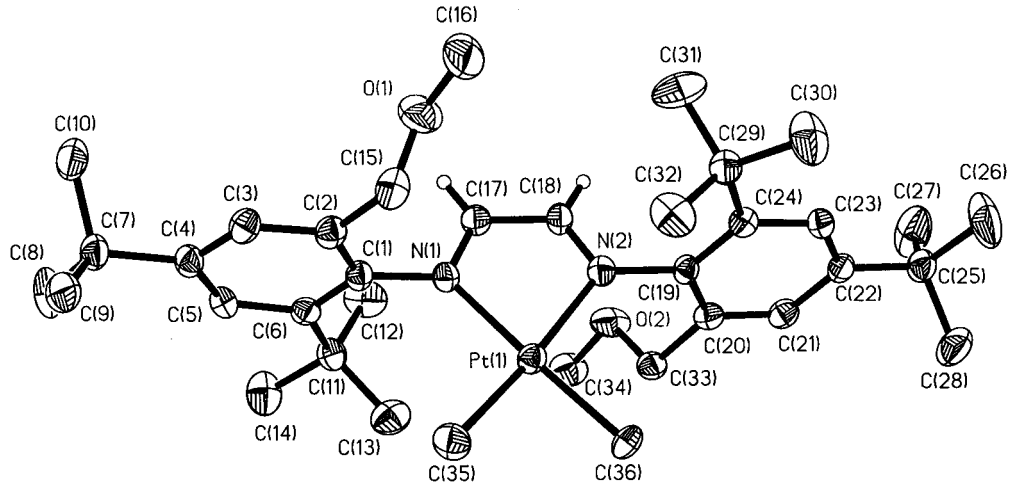

Figure 2. ORTEP diagram of **2b**. Thermal ellipsoids are shown at 50% probability. Hydrogen atoms are omitted for clarity.

Structures of $PtMe_2L$ (2). The structures of both isomers of **2** were determined by single-crystal X-ray diffraction. In each case, single crystals were grown by slow solvent evaporation from saturated hexane solutions at −10 °C. The ORTEP diagrams of **2a** and **2b** are shown in Figures 1 and 2, with details of the structure determination including unit cell data, data collection parameters, and refinement information summarized in Table 3. Relevant bond distances, bond angles, and torsion angles for both structures are presented in Tables 4−6, respectively. Since there are two independent molecules in the asymmetric unit for **2a** and both molecules have almost the same metrical parameters, the ORTEP diagram in Figure 2 is given for one molecule only and the metrical data presented in Tables 4−6 are for the same molecule. Metrical parameters for the second molecule are provided in the Supporting Information.

Both **2a** and **2b** possess slightly distorted square-planar coordination geometries with bond angles deviating from 90° by virtue of the constraints imposed by chelation of **L** (N−Pt−N of 76.0(7) and 77.04 (9)° for **2a** and **2b**, respectively). The observed N−Pt−N bond angles in **2** are slightly but significantly smaller than that of the dichloro derivative **1b** (79.4(2)°), possibly because of the sterically larger methyl groups in **2** relative to the chloride ligands in **1b.** The metal chelate rings in both isomers are essentially planar, as seen from the torsion angles given in Table 6. As in the dichloro derivative **1b**, the aryl rings are almost perpendicular to the chelate rings in **2a** and **2b**, with torsion angles about the imine N−C(ipso) bond of near 90° (see Table 6). The diffraction studies reveal that the relative orientation of the two CH_2OMe groups in **2a** is syn or cisoid (i.e., both on the same side of the coordination plane) while in **2b** the groups are anti or transoid (on opposite sides of the coordination plane). There are no significant differences observed in the Pt−C and Pt−N bond distances between the two isomers, with Pt−C bonds of 2.05(2) and 2.06(2) Å for **2a** and 2.059(3) and 2.079(3) Å for **2b** and Pt−N bonds of 2.09(2) and 2.08(2) Å for **2a** and 2.094(2) and 2.112-(2) Å for **2b**, respectively. The observed Pt−N bond distances in **2a** and **2b** are slightly longer than those in **1b** as a result of the stronger trans influence of the methyl ligands in the former relative to chloride in the latter.[27]

(27) Atwood, J. D. *Inorganic and Organometallic Reaction Mechanisms*; Brooks/Cole: Monterey, CA, 1985.

Table 3. Summary of Crystallographic Data for Complexes 2a,b and 3a

	2a	2b	3a
Crystal Parameters			
chem formula	$C_{36}H_{58}N_2O_2Pt$	$C_{36}H_{58}N_2O_2Pt$	$C_{47}H_{77}ClN_2O_2Pt$
fw	745.93	745.93	932.65
cryst syst	orthorhombic	monoclinic	orthorhombic
space group (No.)	$P2_12_12_1$ (19)	$P2_1/c$ (14)	*Pbca* (61)
Z	8	4	8
a, Å[a]	10.7170(1)	14.4682(2)	22.0854(4)
b, Å	24.3547(1)	18.6177(2)	11.5173(2)
c, Å	28.1395(3)	14.5675(1)	34.7360(7)
β, deg		116.087(0)	
V, Å^3	7344.67(11)	3524.22(7)	8832.8(3)
ρ_{calcd}, g cm^{-3}	1.348	1.406	1.403
cryst dimens, mm^3	0.01 × 0.03 × 0.36	0.04 × 0.18 × 0.24	0.12 × 0.12 × 0.18
temp, °C	−80	−90	−80
Measurement of Intensity Data and Refinement Parameters			
radiation (λ, Å)	Mo Kα (0.710 73)		
2θ range, deg	4−40	3−56.7	3−45
total no. of data	21 730	21 064	11 348
no. of unique data	6748	8193	30 399
R_{int}, R_{sigma} (%)[b]	10.10, 10.35	2.88, 4.00	6.90, 5.37
no. of obsd data ($I > 2\sigma(I)$)	5557	6791	4755
no. of params varied	340	370	494
μ, mm^{-1}	3.851	4.013	3.271
abs cor	empirical (SADABS)[c]		
range of transmission factors	0.928−0.749	0.928−0.720	0.928−0.789
GOF[d]	1.081	1.028	1.191
R1(F_o), wR2(F_o^2) obsd (%)[e]	7.50, 14.62	2.85, 5.58	8.06, 13.10
R1(F_o), wR2(F_o^2) all (%)	9.55, 15.51	4.20, 5.96	10.81, 13.92

[a] It has been noted that the integration program SAINT produces cell constant errors that are unreasonably small, since systematic error is not included. More reasonable errors might be estimated at 10× the listed value. [b] $R_{int} = \sum|F_o^2 - F_o^2\ (mean)|/\sum[F_o^2]$; $R_{sigma} = \sum[\sigma(F_o^2)]/\sum[F_o^2]$. [c] The SADABS program is based on the method of Blessing; see: Blessing, R. H. *Acta Crystallogr., Sect. A* **1995**, *51*, 33. [d] GOF = $[\sum[w(F_o^2 - F_c^2)^2]/(n-p)]^{1/2}$, where n and p denote the number of data and parameters. [e] R1 = $(\sum||F_o| - |F_c||)/\sum|F_o|$; wR2 = $[\sum[w(F_o^2 - F_c^2)^2]/\sum[w(F_o^2)^2]]^{1/2}$, where $w = 1/[\sigma^2(F_o^2) + (aP)^2 + bP]$ and $P = [(\text{Max } 0, F_o^2) + 2F_c^2]/3$.

Isomerization of 2a and 2b. Differences in the ratio **2a**:**2b** at different temperatures during the synthesis of **2** suggested the possibility of an isomerization process occurring under relatively mild thermal conditions. This was confirmed when pure samples of either isomer in either $CDCl_3$ or benzene-d_6 were heated in sealed NMR tubes at 349 K, leading to mixtures of both isomers after several hours (eq 2). Accordingly, the

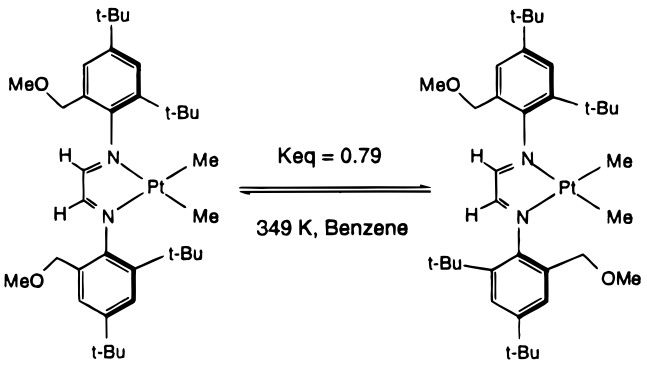

2a **2b** (2)

Table 4. Selected Bond Distances (Å) for 2a,b and 3a

Compound **2a**			
Pt(11)−C(41)	2.05(2)	Pt(11)−C(31)	2.06(2)
Pt(11)−N(11)	2.09(2)	Pt(11)−N(21)	2.08(2)
N(11)−C(11)	1.31(3)	N(11)−C(51)	1.46(3)
N(21)−C(21)	1.25(2)	N(21)−C(111)	1.44(3)
O(21)−C(331)	1.33(3)	O(21)−C(341)	1.39(3)
O(11)−C(351)	1.39(2)	O(11)−C(361)	1.44(3)
Pt(12)−C(32)	2.05(2)	Pt(12)−C(42)	2.06(2)
Pt(12)−N(12)	2.13(2)		
Compound **2b**			
Pt(1)−C(35)	2.059(3)	Pt(1)−C(36)	2.079(3)
Pt(1)−N(1)	2.094(2)	Pt(1)−N(2)	2.112(2)
O(1)−C(15)	1.414(4)	O(1)−C(16)	1.418(4)
O(2)−C(34)	1.421(4)	O(2)−C(33)	1.423(3)
N(1)−C(17)	1.289(3)	N(1)−C(1)	1.438(4)
N(2)−C(18)	1.283(4)	N(2)−C(19)	1.437(4)
C(1)−C(6)	1.398(4)		
Compound **3a**			
Pt(1)−N(1)	1.994(9)	Pt(1)−C(1)	2.053(10)
Pt(1)−N(2)	2.122(9)	Pt(1)−Cl(1)	2.283(3)
O(1)−C(10)	1.400(13)	O(1)−C(11)	1.41(2)
O(2)−C(27)	1.31(2)	O(2)−C(26)	1.395(14)
N(1)−C(2)	1.268(13)	N(1)−C(4)	1.442(13)
N(2)−C(3)	1.280(14)	N(2)−C(20)	1.457(14)
C(2)−C(3)	1.47(2)		

Table 5. Selected Bond Angles (deg) for 2a,b and 3a

Compound **2a**			
C(41)−Pt(11)−C(31)	88.8(8)	N(11)−Pt(11)−N(21)	76.0(7)
C(41)−Pt(11)−N(11)	173.7(8)	C(11)−N(11)−Pt(11)	114.5(14)
C(31)−Pt(11)−N(11)	97.4(8)	C(51)−N(11)−Pt(11)	127(2)
C(41)−Pt(11)−N(21)	97.8(7)	C(21)−N(21)−Pt(11)	114(2)
C(31)−Pt(11)−N(21)	173.4(8)	C(111)−N(21)−Pt(11)	125(2)
Compound **2b**			
C(35)−Pt(1)−C(36)	86.90(13)	N(1)−Pt(1)−N(2)	77.04(9)
C(35)−Pt(1)−N(1)	98.18(12)	C(17)−N(1)−Pt(1)	114.4(2)
C(36)−Pt(1)−N(1)	173.19(10)	C(1)−N(1)−Pt(1)	128.3(2)
C(35)−Pt(1)−N(2)	174.76(11)	C(18)−N(2)−Pt(1)	113.5(2)
C(36)−Pt(1)−N(2)	98.05(11)	C(19)−N(2)−Pt(1)	129.0(2)
Compound **3a**			
N(1)−Pt(1)−C(1)	95.5(4)	N(2)−Pt(1)−Cl(1)	97.3(3)
N(1)−Pt(1)−N(2)	78.1(4)	C(2)−N(1)−Pt(1)	116.4(8)
C(1)−Pt(1)−N(2)	173.4(4)	C(4)−N(1)−Pt(1)	127.6(7)
N(1)−Pt(1)−Cl(1)	175.0(3)	C(3)−N(2)−Pt(1)	112.5(8)
C(1)−Pt(1)−Cl(1)	89.1(3)	C(20)−N(2)−Pt(1)	125.7(7)

interconversion of the two isomers was examined at several different temperatures.[27,28] Figure 3a shows the changes in benzylic ^{1}H resonances for the isomerization of **2a** in benzene-d_6 at 349 K. The equilibrium constant K_{eq} of the isomerization process was determined to be ca. 0.79 from NMR peak integrations of the diimine protons, while the approach to equilibrium, given by the sum of forward and reverse rates $k_1 + k_{-1}$, was ascertained from a first-order plot of $\ln[(C_e - C_o)/(C_e - C_t)]$ vs time (Figure 3b), where C_e is the concentration of **2a** at equilibrium, C_t is the concentration at time t, and C_o is the concentration at time zero. From these values, the forward and reverse rates were calculated, along with their respective free energies of activation, $\Delta G_f^{\ddagger}$ and $\Delta G_r^{\ddagger}$, of 27.0 ± 1.2 and 26.8 ± 1.2 kcal/mol. Measurements of K_{eq} and the sum $k_1 + k_{-1}$ as a function of temperature in order to obtain activation parameters $\Delta H^{\ddagger}$ and $\Delta S^{\ddagger}$ for the isomerization process were not successful because equilibrium concentrations over a large enough temperature range were not accessible,

(28) Bradley, D. H.; Khan, M. A.; Nicholas, K. M. *Organometallics* **1992**, *11*, 2598−2607.

Table 6. Selected Torsion Angles (deg) for 2a,b and 3a

	Compound **2a**		
C(31)−Pt(11)−N(11)−C(11)	172.04(1.63)	Pt(11)−N(11)−C(11)−C(21)	8.83(2.38)
N(21)−Pt(11)−N(11)−C(11)	−7.63(1.51)	C(111)−N(21)−C(21)−C(11)	−175.70(2.05)
C(31)−Pt(11)−N(11)−C(51)	10.25(1.79)	Pt(11)−N(21)−C(21)−C(11)	−2.26(2.65)
N(21)−Pt(11)−N(11)−C(51)	−169.42(1.78)	N (11)−C(21)−C(21)−N(21)	−4.50(3.06)
C(41)−Pt(11)−N(21)−C(21)	−173.42(1.61)	Pt(11)−N(11)−C(51)−C(61)	−99.77(2.47)
N(11)−Pt(11)−N(21)−C(21)	5.17(1.56)	Pt(11)−N(21)−C(111)−C(121)	−88.92(2.26)
C(41)−Pt(11)−N(21)−C(111)	−0.28(1.75)	Pt(11)−N(11)−C(51)−C(101)	78.98(2.38)
N(11)−Pt(11)−N(21)−C(111)	178.31(1.77)	Pt(11)−N(21)−C(111)−C(161)	94.81(2.37)
C(51)−N(11)−C(11)−C(21)	172.55(1.83)		
	Compound **2b**		
C(35)−Pt(1)−N(1)−C(17)	179.71(0.22)	Pt(1)−N(1)−C(1)−C(6)	−94.67(0.30)
N(2)−Pt(1)−N(1)−C(17)	1.89(0.20)	Pt(1)−N(1)−C(1)−C(2)	86.10(0.29)
C(35)−Pt(1)−N(1)−C(1)	4.91(0.26)	Pt(1)−N(1)−C(17)−C(18)	0.08(0.35)
N(2)−Pt(1)−N(1)−C(1)	−172.92(0.25)	Pt(1)−N(2)−C(18)−C(17)	5.08(0.35)
C(36)−Pt(1)−N(2)− C(18)	171.44(0.22)	N(1)−C(17)−C(18)− N(2)	−3.58(0.44)
N(1)−Pt(1)−N(2)−C(18)	−3.77(0.20)	Pt(1)−N(2)−C(19)−C(24)	−101.09(0.30)
C(36)−Pt(1)−N(2)−C(19)	−1.62(0.24)	Pt(1)−N(2)−C(19)−C(20)	80.48(0.30)
N(1)−Pt(1)−N(2)−C(19)	−176.82(0.25)		
	Compound **3a**		
C(1)−Pt(1)−N(1)−C(2)	174.36(0.84)	Cl(1)−Pt(1)−N(2)−C(20)	−3.06(0.87)
N(2)−Pt(1)−N(1)−C(2)	−4.27(0.79)	Pt(1)−N(1)−C(2)−C(3)	2.18(1.29)
C(1)−Pt(1)−N(1)−C(4)	0.31(1.00)	Pt(1)−N(2)−C(3)−C(2)	−6.57(1.22)
N(2)−Pt(1)−N(1)−C(4)	−178.32(1.00)	N(1)−C(2)−C(3)−N(2)	3.28(1.52)
N(1)−Pt(1)−N(2)−C(3)	5.96(0.78)	Pt(1)−N(1)−C(4)−C(5)	82.34(1.22)
C(1)−Pt(1)−N(2)−C(3)	−6.06(3.78)	Pt(1)−N(1)−C(4)−C(9)	−94.74(1.22)
Cl(1)−Pt(1)−N(2)−C(3)	−171.93(0.76)	Pt(1)−N(2)−C(20)−C(25)	96.10(1.20)
N(1)−Pt(1)−N(2)−C(20)	174.83(0.92)	Pt(1)−N(2)−C(20)−C(21)	−79.90(1.18)
C(1)−Pt(1)−N(2)−C(20)	162.81(3.12)		

owing to partial decomposition in benzene-d_6 and slow transformation of **2a**,**b** to the new purple species, **3a**,**b** in $CDCl_3$ (vide infra).

There are two logical pathways for the isomerization of dimethyl complex **2**. The first is via direct rotation about the C(aryl)−N bonds of the coordinated imine groups, while the second involves dissociation of one end of the diazabutadiene ligand from the metal center followed by bond rotation and recoordination. Both pathways possess potentially high activation energies, since the former would involve large steric repulsions between bulky ortho substituents on the aryl rings and the diimine chelate ring while the latter would necessitate dissociation of a Pt−N bond. It is uncertain which pathway is operative for the isomerization at this point, but the information obtained from isomerization of the chloro methyl derivative **3** discussed below favors the mechanism involving hindered rotation about the C(aryl)−N bonds.

Thermolysis of the Dimethyl Complex 2. During the course of investigating the isomerization of **2**, we observed upon heating a $CDCl_3$ solution of the complex for 24 h at 349 K a color change from deep green to purple and the appearance of two new species. Partial decomposition was also seen during this thermolysis, as evidenced by the formation of a black precipitate and ^{1}H NMR resonances of free ligand **L** in addition to those of the new species. TLC analysis of the purple solution showed two spots, and separation of the new products was achieved by preparative TLC on silica using $CHCl_3$ as eluant. Characterization of the new products was achieved by ^{1}H NMR spectroscopy and by an X-ray diffraction study of one of the two products. The similarity of the properties and NMR resonances for the new products indicates that, as in the case of the dimethyl complex **2**, these new species are actually two isomers of a single compound **3** as shown in eq 3.

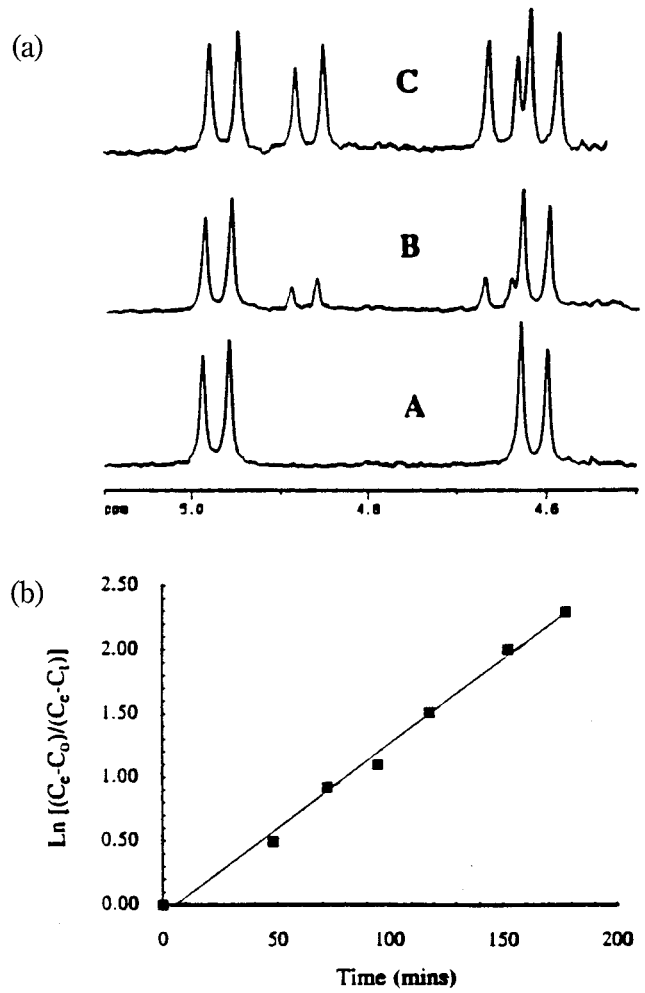

Figure 3. (a) Benzylic proton resonances for the isomerization of **2** at 349 K: (A) t = 0 min; (B) t = 50 min; (C) t = 350 min. (b) First-order plot for the isomerization of **2** at 349 K.

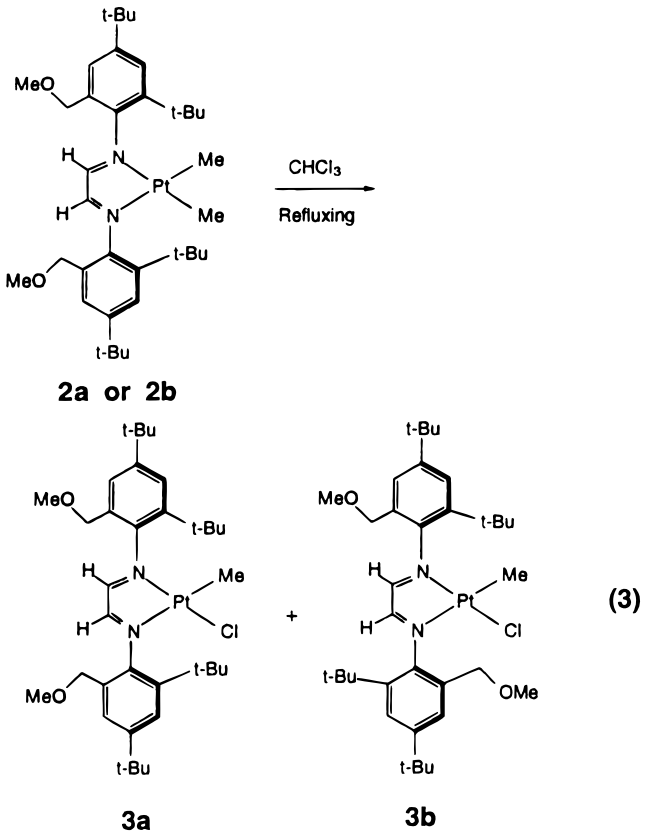

(3)

The ^{1}H NMR spectra of isomers **3a**,**b** in C_6D_6 each show *two* characteristic singlets for the diimine (N=C*H*C*H*=N) protons (δ 7.91, 8.56 for **3a** and δ 7.81, 8.45 for **3b**), *two* resonances for the methoxy protons (δ 3.20, 3.21 for **3a** and δ 3.17, 3.18 for **3b**), four sets of doublets for the benzylic protons, and four *tert*-butyl resonances (δ 1.57, 1.45, 1.31, 1.26 for **3a** and δ 1.62, 1.50, 1.31, 1.26 for **3b**) consistent with an unsymmetrical structure for each of the two isomers (see Table 1). In addition to the diimine, methoxy, and *tert*-butyl protons, each isomer was observed to have only a single Pt-coordinated methyl resonance at δ 2.02 for **3a** and δ 2.00 for **3b**, with J_{Pt-H} coupling constants of 41.2 and 40.8 Hz, respectively. From the single-crystal structure determination discussed briefly below, it was established that **3** corresponds to the chloro methyl complex PtCl(Me)**L**.

Proton decoupling experiments were used to correlate and assign the different benzylic proton resonances. The benzylic proton doublets for **3a** are centered at δ 5.29, 4.82, 4.55, and 4.51, and for **3b** they are at δ 5.20, 4.81, 4.59, and 4.56, with the same J_{H-H} coupling constant of 11.6 Hz for each set. Irradiation of the doublet in **3a** at δ 5.29 results in a singlet at δ 4.55, while irradiation of the doublet at δ 4.82 leads to a singlet at δ 4.51, thus allowing assignment of the protons at δ 5.29 and 4.82 as belonging to one benzylic group and the protons at δ 4.82 and δ 4.51 comprising the other. Similar decoupling experiments were performed to assign the resonances of **3b**.

The ^{13}C NMR spectra of isomers **3a**,**b** (Table 2) in $CDCl_3$ show the Pt−Me carbon resonances at δ −11.7 and −11.6, along with those of 4 *tert*-butyl groups, 2 methoxy groups, 2 benzylic groups, and 12 phenyl carbons (Table 2). The resonances for the diimine carbons are seen at δ 165.7 and 166.6 for **3a** and δ 166.3 and δ 166.5 for **3b**. The observed ^{13}C NMR data are fully consistent with the unsymmetrical nature of **3**.

The chloro methyl complex **3** also isomerizes, but at much lower temperature than the dimethyl complex **2** (eq 4). An NMR tube containing a solution of pure **3a**

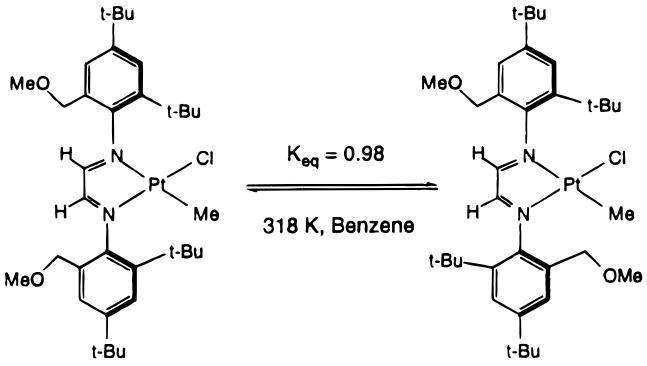

(4)

in benzene-d_6 maintained at ambient room temperature for 24 h leads to a ca. 2:1 mixture of isomers. The isomerization proceeds faster at elevated temperature. Heating a sample of **3a** in benzene-d_6 to 318 K produces a 1:1 mixture of isomers within 2 h. Following the same procedure used to determine the free energy of activation for the isomerization of **2**, the equilibrium constant K_{eq} of the isomerization process of **3** at 318 K was determined to be ca. 0.98 ± 0.05, while the sum of forward and reverse rates, $k_1 + k_{-1}$, was determined to be 4.2×10^{-4} s^{-1} from a first-order plot of ln $[(C_e - C_o)/(C_e - C_t)]$ vs time. From these values, the free energies of activation of the forward and reverse rates, $\Delta G_f^{\ddagger}$ and $\Delta G_r^{\ddagger}$, were calculated to be 24.1 ± 1.2 and 24.0 ± 1.2 kcal/mol, respectively. The $\Delta G^{\ddagger}$ values obtained for the isomerization of PtCl(Me)**L** are ca. 3 kcal/mol lower than those for the isomerization of the corresponding dimethyl analogues **2a**,**b**. The easier isomerization of **3** relative to **2** favors simple rotation of the C(aryl)−N bonds as the mechanism of isomerization since chloride is sterically smaller than methyl, and chloride as a trans ligand is not expected to facilitate diimine dissociation.[27]

The formation of **3** from **2** in chloroform provides an easy entry to chloromethylplatinum(II) derivatives, which serve as convenient precursors for cationic electrophilic species via halide abstraction with silver salts. With regard to the mechanism of formation of **3**, the exchange of one of the methyl groups in **2** for a chloride probably proceeds via a radical pathway. In support of this notion, it has been reported previously that Pt(II) dimethyl diimine complexes undergo free radical oxidative addition reactions with alkyl halides under thermal as well as photochemical conditions.[29]

Structure of PtMeClL (3a). The structure of **3a** was determined by single-crystal X-ray diffraction. Single crystals were grown by the slow diffusion of heptane into a saturated benzene/hexane solution of the complex at −10 °C. The ORTEP diagram of **3a** is shown in Figure 4, with details of the structure determination, including unit cell data, summarized in Table 3 and

(29) Hill, R. H.; Puddephatt, R. J. *J. Am. Chem. Soc.* **1985**, *107*, 1218−1223.

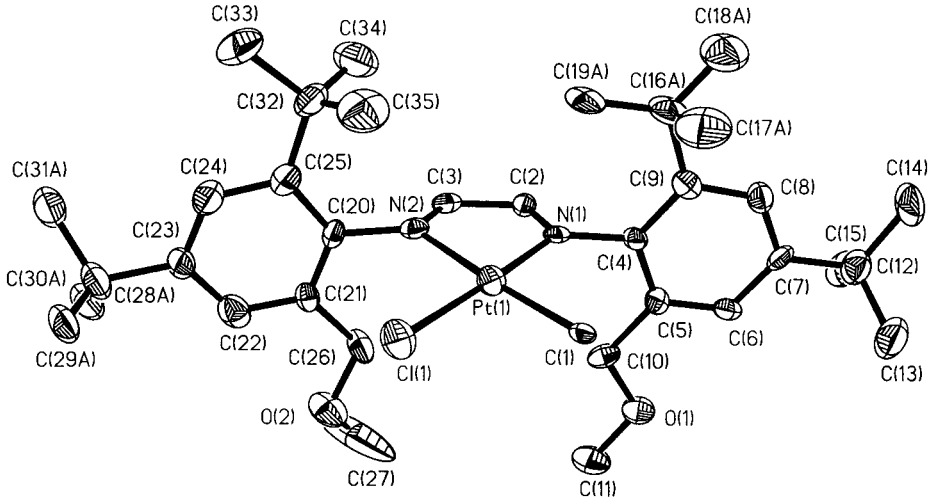

Figure 4. ORTEP diagram of **3a**. Thermal ellipsoids are shown at 50% probability. Hydrogen atoms are omitted for clarity.

relevant bond distances, bond angles, and torsion angles listed in Tables 4−6, respectively.

The chloro methyl compound **3a** possesses a slightly distorted square-planar geometry. The bond angle of 78.1(4)° for N(1)−Pt−N(2) results from the constraints of chelation by **L** and is intermediate between corresponding values for the dimethyl and dichloro complexes. As a consequence of the larger structural trans influence of the Me group relative to chloride, the Pt−N(2) bond is 0.128 Å longer than the Pt−N(1) bond. As seen in the structures of the dichloro derivatives **1a**,**b**, and the dimethyl complexes **2a**,**b**, the two aryl rings of **L** are nearly normal to the coordination plane defined by the metal chelate ring, as a result of steric interactions between the bulky ortho substituents of the aryl rings and the diimine chelate protons. The observed Pt−Cl (2.283(3) Å) and Pt−C (2.053(10) Å) bond distances are comparable to those seen in other platinum diimine complexes.[30,31]

Halide Abstraction and the Generation of Cationic Complexes. Synthesis of [PtMeL(MeCN)][BF$_4$] (4). The chloro methyl complex **3** (1:1 mixture of isomers **3a**,**b**) reacts with 1.05 equiv of silver tetrafluoroborate in acetonitrile to give the cationic solvento complex [PtMeL(MeCN)][BF_4] (**4**) in good yield (eq 5). As with **2** and **3**, two isomers of **4** are obtained in a 1:1 ratio. Purification of **4** is achieved by initial removal of the silver chloride precipitate and subsequent recrystallization from hexane/CH_2Cl_2 (5:1 v/v).

Characterization of **4** by ^{1}H NMR spectroscopy in $CDCl_3$ reveals two singlets at δ 2.03 and 2.04 for coordinated acetonitrile (Table 1). The presence of a separate resonance at δ 2.00 for free acetonitrile indicates that any acetonitrile exchange in chloroform is in the slow exchange limit (10 s^{-1}). In addition to the coordinated acetonitrile resonances for the two isomers of **4**, the ^{1}H NMR spectrum shows resonances for four methoxy groups (δ 3.29, 3.33, 3.35, 3.37), four diimine protons (δ 8.99, 9.01, 9.05 (2H)), and two Pt-bound Me groups (δ 0.79, 0.80). Additionally, the eight CH_2 resonances of the methoxymethyl groups are seen but cannot be resolved because of overlap. In the ^{13}C NMR spectrum of **4**, both isomers give the same chemical shift at δ 119.2 for the acetonitrile nitrile carbon.

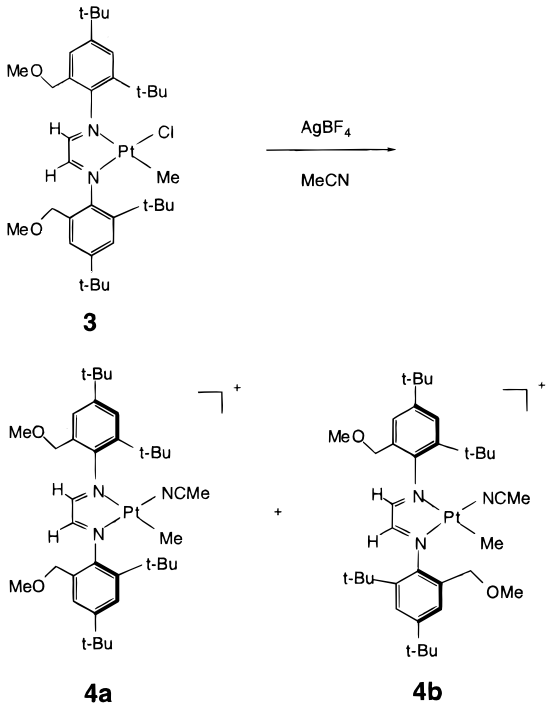

(5)

The existence of slow acetonitrile exchange involving **4** was established by dissolving a sample of the complex in CD_3CN for 1 h, isolating it, and then measuring its ^{1}H NMR spectrum in $CDCl_3$. The spectrum of this sample showed that MeCN had been completely exchanged with CD_3CN, by the disappearance of resonances at δ 2.03 and 2.04, while other features of the spectrum remained identical with those described above for **4**. By the same procedure, coordinated CD_3CN was completely exchanged by CH_3CN, showing that the exchange process, while slow, is fully reversible. The slowness of the acetonitrile exchange in **4** may be attributed to the steric bulk of the ortho substituents on the diaryldiazabutadiene ligand **L** and consequent

(30) Wilkinson, G.; Stone, F. G. A.; Abel, E. W. *Comprehensive Organometallic Chemistry: The Synthesis, Reactions and Structures of Organometallic Compounds*; Wilkinson, G., Stone, F. G. A., Abel, E. W., Eds.; Pergamon Press: Elmsford, NY, 1982; Vol. 6.
(31) De Felice, V.; Ganis, P.; Vigaliano, A.; Valle, G. *Inorg. Chim. Acta* **1988**, *144*, 57−61.

inhibition of associative substitution paths that involve addition from above or below the coordination plane.

Synthesis of [PtMeL(pyr)][BF_4] (5). The pyridine-coordinated complex **5** was prepared by dissolving **4** in neat pyridine and stirring for 1 h. The procedure was the same as that used to prepare the CD_3CN-coordinated complex **4** (vide supra). The key features in the ^1H NMR spectrum of **5** are very similar to those of acetonitrile complex **4** (see Table 1), except for the coordinated pyridine resonances in the region between δ 6.8 and 8.2, which are overlapped with those of the phenyl protons on **L**.

Halide Abstraction in the Presence of Olefins. Syntheses of [PtMeL(C_2H_3R)][BF_4] with R = H, CN. The preparation of α-olefin complexes of the formula [PtMeL(C_2H_3R)][BF_4] (R = H, CN) was explored by both acetonitrile displacement from **4** and halide abstraction from **3** in the presence of olefins. The former was carried out in olefin-containing dichloromethane or chloroform solution. Monitoring these reactions by ^1H NMR spectroscopy revealed that acetonitrile displacement by dissolved olefin is very slow. The reaction between **4** and excess acrylonitrile in $CDCl_3$ required 48 h to complete, while the reaction with ethylene was only 5−10% complete after the same amount of time. The acetonitrile displacement route was therefore not pursued further in the synthesis of cationic olefin complexes.

The halide abstraction reaction proved to be much more effective. Treatment of a dichloromethane solution of the chloro methyl complex **3** with 1.05 equiv of $AgBF_4$ salt in the presence of olefins led to the formation of cationic olefin complexes **6** and **7** for ethylene and acrylonitrile, respectively, as red solids in good yields (eq 6). In these reactions, filtration of the reaction

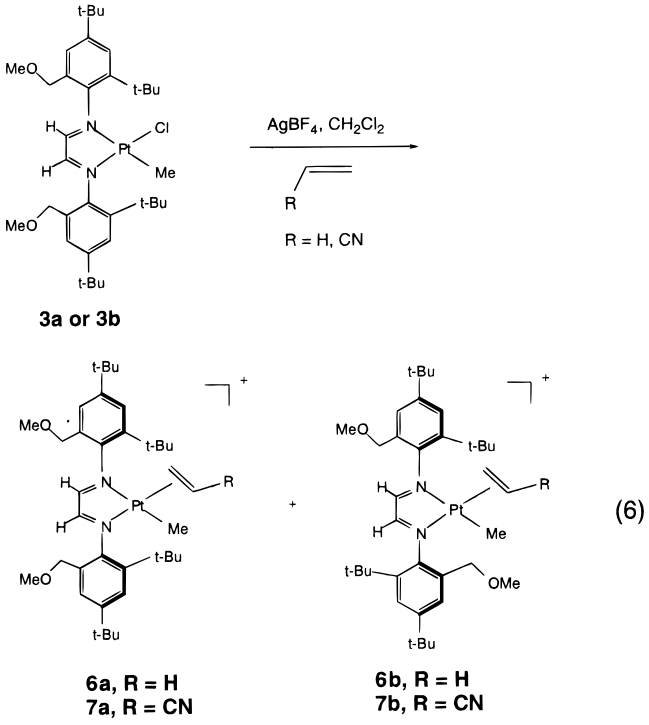

(6)

mixture through Celite, followed by precipitation of the crude product with hexane, gave olefin complexes as red solids. Analytically pure samples of **6** and **7** were obtained by recrystallization three times from a solvent mixture of dichloromethane and hexane (1:3 v/v). Regardless of which isomer of the chloro methyl complex **3** was used for the preparation, olefin complexes **6** and **7** were obtained as 1:1 mixtures of syn and anti isomers. Both complexes are very soluble in dichloromethane, chloroform, and toluene, are insoluble in hydrocarbons, and are air- and moisture stable both in the solid state and in solution.

The cationic olefin complexes **6** and **7** were characterized by both ^1H and ^{13}C NMR spectroscopy. In comparison with acetonitrile complex **4**, complexes **6** and **7** show very similar spectroscopic features except for those of the coordinated olefins (Tables 1 and 2). While the ^1H NMR spectrum of ethylene complex **6** is not very informative because of overlap of resonances for ethylene and benzylic protons, the ^{13}C NMR spectrum in $CDCl_3$ clearly shows the coordinated ethylene at δ 74.29 and 74.32 ppm with the same J_{Pt-C} coupling of 99 Hz for the two isomers of **6** having syn and anti orientations of the methoxymethyl and *tert*-butyl substituents. Complex **7** shows the coordinated acrylonitrile at δ 5.7 (multiplets, 4H), 6.23 (d, J_{H-H} = 12 Hz, 1H), and 6.22 (d, J_{H-H} = 12 Hz, 1H) in its ^1H NMR spectrum. The ^1H resonances for the geminal and trans protons of bound olefin in the two isomers **7a**,**b** overlap, while the cis proton resonances are just resolved. In the ^{13}C NMR spectrum, overlap of bound olefin resonances is also seen at δ 105.2 and 144.4, with the third acrylonitrile resonance for **7a**,**b** just resolved at δ 117.4 and 117.5. In accord with this view, the resonances at δ 105.2 and 144.4 appear to correspond to two carbons each, on the basis of a qualitative assessment of resonance intensities. Assignment of the acrylonitrile ^{13}C resonances was made (see Table 2) on the basis of a ^1H-coupled ^{13}C spectrum and the attached proton test (the *J*-modulated spin−echo experiment) for free acrylonitrile. In the ^1H NMR spectrum, comparison of coordinated and free acrylonitrile in $CDCl_3$, the latter occurring at δ 6.21 (J_{H-H} = 16 Hz), δ 6.06 (J_{H-H} = 12 Hz), and δ 5.64 (dd, J_{H-H} = 12 Hz, J_{H-H} = 16 Hz), reveals that only the middle of the three protons in acrylonitrile is shifted significantly upon coordination. The observed chemical shifts for coordinated olefins here are comparable to those of other structurally characterized phenathroline- and diimine-based cationic olefin complexes.[32]

The observation of two ethylene ^{13}C resonances for **6** and two acrylonitrile resonances for **7** in both ^1H and ^{13}C NMR spectra is consistent with the cationic olefin complexes existing as mixtures of isomers that interconvert slowly, if at all. The fact that only a single ^{13}C resonance is seen for ethylene in each isomer of **6** while only three ^{13}C resonances occur for acrylonitrile in each isomer of **7** indicates that the coordinated olefins in **6** and **7** rotate rapidly about the Pt−alkene bond. For **7**, evidence for hindered rotation about the metal−alkene bond in the guise of different conformers for each isomer is not observed.

Exchange of olefins occurs slowly from **6** and **7**. While the addition of free ethylene to a solution of **6** or the addition of acrylonitrile to a solution of **7** has no observable effect on coordinated olefin resonances, olefin

(32) Fusto, M.; Giordano, F.; Orabona, I.; Ruffo, F. *Organometallics* **1997**, *16*, 5981−5987.

exchange can be effected by using neat olefin as solvent. When ethylene complex **6** is dissolved in neat acrylonitrile, complete displacement of the olefin is noted with the formation of **7**. For both **6** and **7**, displacement of the olefin is seen when the complex is dissolved in acetonitrile, leading to the formation of **4**.

Recently, Ruffo and co-workers have reported similar cationic methyl olefin complexes of Pt containing diazabutadiene ligands.[32,33] The DAB ligands are identical with the ones used by Brookhart in which the aryl groups have the same substituents in the 2- and 6-positions. In Ruffo's studies, the cationic methyl olefin complexes were generated either by alkylation of a Pt(0) olefin precursor using OR_3^+ or, as in the present study, by chloride ion abstraction from the corresponding chloro methyl complex with $AgBF_4$ in the presence of olefin. A crystal structure of the η^2-C_2H_4 complex with ethyl groups in the 2,6-positions shows that the olefin is oriented perpendicular to the coordination plane.[32] A connectivity-quality structure of the methyl acrylate derivative reveals a similar orientation.[33] In accord with our conclusions for **6** and **7**, the occurrence of ^{195}Pt satellites in the ^{13}C resonances of the bound olefin indicates that intermolecular exchange of olefin is slow in these systems.

Synthesis of [PtMeL(C_2H_3R)][MeB(C_6F_5)$_3$] (R = H (8), CN (9)). Following Puddephatt's precedent in Pt chemistry for methyl group abstraction using strong Lewis acids, we find that the cationic olefin complexes can also be generated by reacting dimethyl complex **2** with $B(C_6F_5)_3$ in dichloromethane solutions in the presence of olefins (eq 7). For ethylene complex **6**, a sample of **2** and $B(C_6F_5)_3$ in an NMR tube was placed under an ethylene atmosphere and then dissolved in ethylene-degassed $CDCl_3$. For acrylonitrile complex **7**, a sample of **2** and $B(C_6F_5)_3$ was treated with a $CDCl_3$ solution containing a stoichiometric excess of acrylonitrile. For both reactions, the green color of the starting material **2** diminished quickly and the solution acquired a red-orange color. The ^{1}H NMR spectrum of [*cis*-PtMeL(C_2H_3CN)]$^+$ [MeB(C_6F_5)$_3$] clearly shows the proton resonances of coordinated acrylonitrile at δ 6.23 (J_{HH} = 12 Hz), δ 5.81 (J_{HH} = 16 Hz), and δ 5.60 (J_{HH} = 12 Hz). However, the observed resonances of coordinated acrylonitrile for both isomers are not well-resolved, with lines somewhat broader than those of free acrylonitrile. While the coordinated acrylonitrile does not provide evidence of two different isomers for **9**, the resonances of ligand **L** clearly do. The differences in the coordinated acrylonitrile resonances between **7** and **9** may be attributable to the different modes of preparing [Pt(Me)(CH_2=CHCN)**L**]$^+$ and the resultant different counterions.

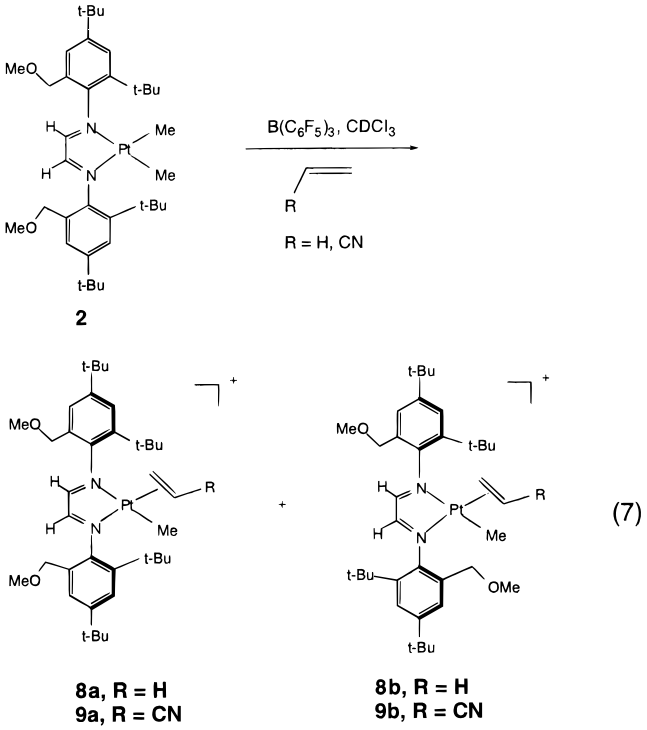

(7)

Conclusion

New dimethyl, chloro methyl, and cationic platinum complexes of the bulky diazabutadiene ligand **L** have been synthesized and characterized. The 2,6-aryl substituents of the ligand **L** effectively block facile rotation about the imine N−C(ipso) bond, leading to the observed formation and isolation of two isomers for each complex. The structures of the complexes have been shown by X-ray crystallography and NMR spectroscopy to contain square-planar-coordinated Pt(II) ions with the isomers differing in the relative orientation of the methoxymethyl and *tert*-butyl substituents of the aryl groups with respect to the coordination plane. For the dimethyl complex $PtMe_2$**L** (**2**), the two isomers possess C_s and C_2 symmetries. Interconversion of the isomers occurs slowly for $PtMe_2$**L** and more rapidly for the chloro methyl system PtClMe**L** (**3**), consistent with a simple hindered rotation process. Cationic monomethyl complexes have been synthesized by chloride ion abstraction using $AgBF_4$, which in the presence of ethylene or acrylonitrile leads to the olefin complexes [PtMe(C_2H_4)**L**]$^+$ and [PtMe(C_2H_3CN)**L**]$^+$. These same complexes have also been prepared in situ by methyl group abstraction from dimethyl complex **2** using the strong Lewis acid $B(C_6F_5)_3$ in dichloromethane. The exchange processes between coordinated MeCN, CD_3CN, and olefins in the cationic monomethyl complexes have also been demonstrated. The reactivities of the cationic solvento complexes toward C−H activation reactions is currently under investigation and the results will be reported in due course.

Experimental Section

Procedures and Materials. The 1,4-diazabutadiene ligand glyoxal bis(2-(methoxymethyl)-4,6-di-*tert*-butylphenyl)diimine (**L**) was prepared by following the published procedure.[26] The complex $Pt_2Me_4(SMe_2)_2$ was prepared by a modification of the procedure by Elsevier.[24] The reagents $AgBF_4$ and $B(C_6F_5)_3$ were purchased from Strem and used as received. Unless otherwise noted, all reactions and manipulations were performed in dry glassware under a nitrogen atmosphere using either standard Schlenk techniques or an inert-atmosphere glovebox. All NMR spectra were recorded on a Bruker AMX 400 MHz spectrometer. Proton homonuclear decoupling experiments were performed using the pulse program HOMO-

(33) Ganis, P.; Orabona, I.; Ruffo, F.; Vitagliano, A. *Organometallics* **1998**, *17*, 2646−2650.

DEC. Elemental analyses were obtained from Quantitative Technologies, Inc., Whitehouse, NJ.

Synthesis of $PtMe_2L$ (2a,b). To a 50 mL Schlenk flask containing 20 mL of CH_2Cl_2 was added 0.10 g (0.19 mmol) of glyoxal bis(2-(methoxymethyl)-4,6-di-*tert*-butylphenyl)imine (**L**) and 0.10 g (0.18 mmol) of $Pt_2Me_4(SMe_2)_2$, after which the reaction solution was stirred for 48 h at room temperature. The color of the reaction solution slowly changed from yellow to deep green. The solvent was removed by vacuum, and the residue was separated by column chromatography using a 9:1 mixture of CH_2Cl_2 and hexane on silica gel. Yield: **2a**, 0.01 g (7.5%); **2b**, 0.05 g (38%). The low yields are caused by partial decomposition of the product during chromatographic separation, with decomposed material giving a red color on the column. Anal. Calcd for **2a** ($C_{36}H_{58}N_2O_2Pt$): C, 57.96; H, 7.84; N, 3.75. Found: C, 57.91; H, 7.91; N, 3.47. Calcd for **2b** ($C_{36}H_{58}N_2O_2Pt$): C, 57.96; H, 7.84; N, 3.75. Found: C, 57.89; H, 7.92; N, 3.44.

Isomerization of 2a and 2b. An NMR tube containing 0.8 mL of a 13.8 mM benzene-d_6 solution of either **2a** or **2b** was maintained at the desired temperature, and ^{1}H NMR spectra were taken at specified time intervals. The reaction profile was determined by plotting the relative integrations of **2a** and **2b** versus time. Slight decomposition of both isomers was noted when the NMR tube was maintained at temperatures above 323 K for longer than 6 h. The equilibrium constant K_{eq} of the isomerization process was determined to be ca. 0.79 from NMR peak integrations of the diimine protons, while the sum of forward and reverse rates, $k_1 + k_{-1}$, was determined by a first-order plot of ln $[(C_e - C_o)/(C_e - C_t)]$ vs time, where C_e is the concentration of **2a** at equilibrium, C_t is the concentration at time t, and C_o is the concentration at time zero (Figure 3).

Synthesis of PtMeClL (3a,b). A 50 mL Schlenk flask was charged with 0.13 g (0.17 mmol) of **2** and 20 mL of $CHCl_3$, and the solution was heated to reflux for 24 h. The color of the reaction solution changed slowly from deep green to purple. The reaction was monitored by NMR and TLC analysis until **2** was no longer present in the reaction solution. The solvent was removed by vacuum, and the residue was separated by preparative TLC using $CHCl_3$ as eluant. Yield: **3a**, 0.025 g (19%); **3b**, 0.017 g (13.1%). The low yields are caused by partial decomposition of the product complex during column separation. Anal. Calcd for **3a** ($C_{35}H_{55}O_2N_2PtCl$): C, 54.85; H, 7.23; N, 3.65. Found: C, 54.79; H, 7.28; N, 3.45 (**3a** and **3b** were analyzed as a mixture since recrystallizations of either isomer resulted in a mixture of both isomers as confirmed by ^{1}H NMR spectroscopy).

Synthesis of $[PtMeL(MeCN)]BF_4$ (4a,b). To a 50 mL Schlenk flask containing 20 mL of MeCN was added 0.10 g (0.13 mmol) of chloro complex **3** and 1.05 equiv of $AgBF_4$. The resulting reaction mixture was monitored by TLC analysis until the purple color of the chloromethyl complex **3** was no longer seen (2 h). The solvent was removed by vacuum, and the solid residue was redissolved into 10 mL of dichloromethane and the solution filtered. Crude product **4** was precipitated by adding hexane to the above filtrate. An analytically pure sample was obtained by recrystallizing the crude product from a solvent mixture of dichloromethane and hexane (1:5 v/v). **4** was obtained as a mixture of two isomers (**4a**,**b**), and attempts to isolate both isomers via fractional recrystallization were unsuccessful. Yield: 0.08 g (72%). Anal. Calcd for **4** ($C_{37}H_{58}BF_4N_3O_2Pt\cdot CH_2Cl_2$): C, 48.36; H, 6.41; N, 4.45. Found: C, 48.95; H, 6.60; N, 4.52.

Exchange of MeCN with CD_3CN in $[PtMeL(MeCN)]BF_4$. To an NMR tube containing 3.5 mg of $[PtMeL(MeCN)]BF_4$ (**4**) was added 0.3 mL of CD_3CN by syringe. The solution was then maintained at room temperature for 1 h. After removal of solvent, the residue was redissolved in 0.8 mL of $CDCl_3$ and its ^{1}H NMR spectrum taken. The spectrum revealed complete replacement of MeCN in **4** by CD_3CN. Exchange of CD_3CN from this sample can be achieved by dissolution in CH_3CN for 1 h.

Synthesis of $[PtMeL(pyr)]BF_4$ (5). Complex **5** was generated in an NMR tube and characterized by ^{1}H NMR spectroscopy. The complex $[PtMeL(MeCN)]BF_4$ (**4**) (10 mg) was dissolved in 0.5 mL of pyridine in an NMR tube and the solution then maintained at room temperature for 1 h. The solvent was next removed under vacuum and the residue was redissolved in 0.8 mL of $CDCl_3$. The spectroscopic data of complex **5** is presented in Table 1.

Synthesis of $[PtMeL(C_2H_4)]BF_4$ (6). A solution of 0.10 g (0.13 mmol) of the chloromethyl complex **3** in 20 mL of CH_2Cl_2 was degassed with ethylene for about 5 min and then treated with 1.05 equiv of $AgBF_4$. The color of the reaction mixture changed slowly from purple to red-brown. The reaction mixture was kept under ethylene and stirred overnight. The product was isolated by filtering the reaction mixture through a short Celite column and then adding hexane to effect product precipitation. The sample of **6** was recrystallized from a solvent mixture of CH_2Cl_2 and hexane (2:8 v/v). Yield: 0.08 g (74%). Anal. Calcd for **6** ($C_{37}H_{59}BF_4N_2O_2Pt$): C, 52.54; H, 7.03; N, 3.31. Found: C, 50.90; H, 6.74; N, 3.17.

Synthesis of $[PtMeL(C_2H_3CN)]BF_4$ (7). A solution was made of 0.10 g (0.13 mmol) of chloromethyl complex **3** and 0.2 mL of acrylonitrile in 20 mL of CH_2Cl_2. The mixture was treated with 1.05 equiv of $AgBF_4$ and was stirred overnight. Purification was achieved by following the same procedure as used for **6**. Yield: 0.082 g (73%). Anal. Calcd for **7** ($C_{38}H_{58}BF_4N_3O_2Pt$): C, 52.41; H, 6.71; N, 4.83. Found: C, 52.77; H, 6.75; N, 4.45.

Displacement of Ethylene by Acetonitrile and Acrylonitrile from $[PtMeL(CH_2CH_2)]BF_4$. To an NMR tube containing 3.5 mg of $[PtMeL(CH_2CH_2)]BF_4$ (**6**) was added 0.3 mL of acetonitrile (or acrylonitrile) by syringe. The solution was maintained at room temperature for 1 h. All volatiles were next removed by vacuum, and the residue was redissolved in 0.8 mL of $CDCl_3$ and its ^{1}H NMR spectrum recorded. The ^{1}H NMR spectrum revealed that ethylene in **6** had been completely replaced by acetonitrile (or acrylonitrile), generating **4** (or **7**).

Synthesis of $[PtMeL(C_2H_4)][MeB(C_6F_5)_3]$ (8). Chloroform saturated with ethylene (0.7 mL) was added to an NMR tube containing **2** (10 mg, 0.015 mmol) and $B(C_6F_5)_3$ (8 mg, 0.016 mmol) under an ethylene atmosphere. The color of the solution quickly changed from green to red-orange. The solution was maintained at room temperature for an additional 20 min, and the formation of the cationic ethylene complex as its $MeB(C_6F_5)_3^-$ salt was confirmed by ^{1}H NMR spectroscopy.

Synthesis of $[PtMeL(C_2H_3CN)][MeB(C_6F_5)_3]$ (9). A procedure analogous to that used for the generation of ethylene complex **8** was employed to prepare the acrylonitrile complex **9.** A stock solution of acrylonitrile in $CDCl_3$ (0.7 mL) was added to an NMR tube containing **2a** (10 mg, 0.015 mmol) and $B(C_6F_5)_3$ (8 mg, 0.016 mol). The color of the solution changed from green to red-orange quickly. The solution was maintained at room temperature for an additional 20 min, and the formation of the acrylonitrile complex was confirmed by ^{1}H NMR spectroscopy.

X-ray Crystallography. Crystals of **2a**,**b** and **3a** were each mounted under Paratone-8277 on glass fibers or in a loop and immediately placed on the X-ray diffractometer in a cold nitrogen stream supplied by a Siemens LT-2A low-temperature device. The X-ray intensity data were collected on a standard Siemens SMART CCD area detector system equipped with a normal-focus molybdenum-target X-ray tube operated at 2.0 kW (50 kV, 40 mA). A total of 1321 frames of data (1.3 hemispheres) were collected using a narrow frame method with scan widths of 0.3° in ω and exposure times of 30 s/frame for **2a**,**b** and **3a** using a crystal-to-detector distance of 5.094 cm (maximum 2θ angle of 56.52°). The total data collection time was approximately 12 h for each crystal. Frames for **2a**,**b**

and **3a** were integrated with the Siemens SAINT program. The unit cell parameters, provided in Table 3, were based upon the least-squares refinement of three-dimensional centroids of >1500 reflections for each crystal. Data were corrected for absorption using the program SADABS.

The space group assignments were made on the basis of systematic absences and intensity statistics by using the XPREP program (Siemens, SHELXTL 5.04).[34] The structures were solved by employing Patterson interpretation and difference Fourier methods for **2a** and by using direct methods for **2b** and **3a**, and all structures were refined by full-matrix least squares on F^2. For Z values of 8 for **2a**, 4 for **2b**, and 8 for **3a**, there are two independent molecules for **2a**, one independent molecule for **2b**, and one independent molecule plus one benzene solvate at full occupancy and half of a half-occupied hexane for **3a** in the asymmetric unit. All of the atoms were refined isotropically for **2a**, except for the platinum atoms, which were refined with anisotropic thermal parameters. All non-hydrogen atoms for **2b** and **3a** were refined anisotropically. All hydrogens were included in idealized positions. Pertinent crystallographic data and experimental conditions are summarized in Table 3.

(34) Intensity statistics from CCD data sets are often unreliable, especially for weakly diffracting crystals.

Acknowledgment. We wish to thank the National Science Foundation (Grants CHE 94-04991 and 97-29311) for support of this work and Alfa/Aesar Johnson Matthey Co. Inc. for a generous loan of platinum salts. We also thank Mr. Paul Albietz for help with the paper and the *J*-modulated spin−echo spectrum of acrylonitrile.

Supporting Information Available: Tables of data collection and refinement parameters, refined positional parameters and equivalent isotropic temperature factors, anisotropic thermal parameters, calculated hydrogen positional parameters, and complete bond distances and angles for non-hydrogen atoms for compounds **2a**,**b** and **3a** (28 pages). Ordering information is given on any current masthead page.

OM980551M